NACA TN 4001 10330

TECH LIBRARY KAFB, NM
0067071

NATIONAL ADVISORY COMMITTEE FOR AERONAUTICS

TECHNICAL NOTE 4001

SOME CONSIDERATIONS OF HYSTERESIS EFFECTS ON TIRE MOTION AND WHEEL SHIMMY

By Robert F. Smiley

Langley Aeronautical Laboratory
Langley Field, Va.

Washington

June 1957

AFMDC
TECHNICAL LIBRARY
AFL 2811

TECH LIBRARY KAFB, NM
0067071

1B

NATIONAL ADVISORY COMMITTEE FOR AERONAUTI(

TECHNICAL NOTE 4001

SOME CONSIDERATIONS OF HYSTERESIS EFFECTS ON TIRE MOTION AND WHEEL SHIMMY

By Robert F. Smiley

SUMMARY

A theoretical study is made of the influence of tire hysteresis effects on the rolling motion and wheel shimmy of landing gears. The results of this study indicate that hysteresis forces and moments have a noticeable secondary influence on the landing-gear rolling behavior. Comparisons of the available experimental data with the corresponding theoretical predictions provide a fair confirmation of the theory.

INTRODUCTION

In reference 1 it was suggested that tire hysteresis effects might be of some importance for explaining the discrepancies that exist between predictions of wheel-shimmy theories and experimental observations. Also, some approximate calculations, based on two different theories of hysteresis effects (theories of refs. 1 and 2), were shown to support this suggestion. However, even though both of these hysteresis theories yielded some results in fairly good agreement with the available experimental data, they are both based, in part, on reasoning that is considered too crude to inspire confidence in the use of either theory for practical purposes. For example, the analysis of reference 1 was based largely on considerations of the hysteresis properties of a standing tire and did not take into account either the rolling velocity or the interaction between tire lateral distortion and twist. The analysis of reference 2 is of value mostly as a qualitative study of the hysteresis phenomena; the final equations presented apparently were intended to apply only to the simplest case of wheel shimmy, and, even for this case, the rational basis for these equations is not evident.

The purpose of the present paper is to provide an improved representation of tire hysteresis forces and moments for use in the analysis of tire motion problems, particularly for wheel shimmy. Another purpose is to illustrate the importance of the hysteresis effects for a simple case of wheel shimmy.

The present analysis is essentially an extension of the analysis of reference 1 to take into account the effects of rolling velocity and interaction between tire lateral distortion and twist on the hysteresis forces and moments. It is based on the same concepts of tire distortion as were used in the previous paper. These concepts are briefly outlined in the present paper. For a more thorough discussion of these concepts, see reference 1.

The present paper is arranged as follows. First, equations are derived for the hysteresis forces and moments acting on a standing or rolling tire. Then, in order to establish the importance of the hysteresis effects, the hysteresis equations are applied to two special cases of wheel motion. One case is for general shimmying motion of an untilted wheel for conditions where the wavelength of any lateral or torsional oscillation is large in comparison with the tire dimensions, and the other case is for wheel shimmy where the wheel has only one degree of freedom, namely, rotation about an inclined swivel axis. The equations of motion and stability conditions for the latter case are developed in appendix A. For both cases some comparisons between theory and experiment are shown and these comparisons roughly confirm the theory. In addition, for the latter case, the results of a few theoretical calculations are presented to illustrate the influence of hysteresis forces and moments on the damping required to stabilize the motion of a hypothetical landing gear.

SYMBOLS

a	trail (perpendicular distance between ground-contact center point and swivel axis)
c_γ	change in lateral distance of center of pressure of vertical force from XZ-plane per radian of lateral wheel tilt
c_λ	change in lateral distance of center of pressure of vertical force from XZ-plane per unit of λ_0
D	differential operator with respect to distance, d/dx or $v^{-1}D_t$
D_t	differential operator with respect to time, d/dt or vD
f	frequency, $\nu/2\pi$

F	lateral hysteresis force
F_0, F_1, F_2	lateral hysteresis forces acting on three different parts of tire
$F_{y,h}$	total lateral hysteresis force acting on tire
$F_{y,s}$	lateral spring force acting on tire
$F_{y,\lambda}$	combined lateral spring and hysteresis force acting on tire
F_z	vertical ground force acting on tire
g	linear (viscous) damping coefficient of shimmy damper (Damping moment = $gD_t\psi$)
G_1, G_2, G_3	coefficients defined by equations (A7a)
h	half-length of ground-contact area
H_1, H_2, H_3	coefficients defined by equations (A7a)
I_ψ	moment of inertia of swiveling part of a landing gear about swivel axis
j	horizontal distance forward of wheel axle
j_1, j_2	horizontal distances of centers of pressure of forces F_1 and F_2 from wheel axle
K	tire constant, $Lk\sqrt{v^2 + \frac{v^2}{L^2}}$
K_α	torsional spring constant of a standing tire
$K_{\alpha,r}$	effective torsional spring constant of a rolling tire
K_γ	lateral tire force due to tilt per radian of tilt angle
K_λ	lateral spring constant of a standing tire

k	equivalent viscous damping coefficient of tire per unit circumferential distance
$l_0, l_1, \ldots l_n$	tire constants, $l_n = \frac{(nL + h)h^{n-1}}{-n!}$
L	relaxation length
M_h	hysteresis moment about swivel axis
$M_{z,h}$	hysteresis moment about a vertical axis through wheel center point
$M_{z,s}$	spring moment about a vertical axis through wheel center point
$M_{z,\alpha}$	combined spring and hysteresis moment about a vertical axis through wheel center point
M_0, M_1, M_2	hysteresis moments corresponding to hysteresis forces F_0, F_1, and F_2
p_1, p_2	functions defined by equations (A23), (A25), and (A26)
$p_{1\infty}, p_{2\infty}$	functions defined by equations (A19)
q	phase angle between lateral deflection and swivel angle
r	free tire radius
s	circumferential coordinate on tire (fig. 1)
S	wavelength, $2\pi/\nu_1$

t	time
v	rolling velocity (assumed to be a constant)
x	horizontal distance parallel to mean direction of rolling motion
X,Y,Z	space-fixed coordinate axes; X-axis is horizontal and parallel to mean direction of rolling motion, Z-axis is vertical, and Y-axis is perpendicular to XZ-plane; XY-plane is ground plane
y_0	lateral deflection of tire equator from XZ-plane at center of ground-contact area
α	twist in tire, radians unless otherwise stated
ζ	tire constant, $1 - \frac{\eta_\lambda K_\lambda h^3}{3(L + h)\eta_\alpha K_\alpha}$
η_x	fore-and-aft hysteresis-force parameter
η_z	vertical-hysteresis-force parameter
η_λ	lateral-hysteresis-force parameter
η_α	hysteresis-moment parameter
η_0	lateral deflection of center plane of wheel with respect to XZ-plane, measured in XY-plane at position corresponding to center of ground-contact area
θ	angle of rotation of wheel about vertical Z-axis, radians
κ	inclination of swivel axis, radians (fig. 2)

$\lambda, \lambda_0, \lambda_1, \lambda_2$ lateral distortion of tire equator with respect to solid parts of wheel; subscript 0 refers to center of ground-contact area, subscript 1 refers to foremost point of ground-contact area, and subscript 2 refers to rearmost point of ground-contact area

ν circular frequency of shimmy oscillations, radians per second, $2\pi f$ or $\nu_1 v$

ν_1 path frequency of shimmy oscillations, νv^{-1}

ξ tire tilt parameter $(0 < \xi < 1)$

ρ spring constant for a linear restoring moment about swivel axis

$$\rho_\kappa = \left(aK_\gamma - aF_z + ac_\lambda F_z + c_\gamma F_z \sin \kappa\right) \sin \kappa$$

$$\sigma = 1 + \xi Lh \frac{\tan \kappa}{l_1 r}$$

τ tire parameter associated with gyroscopic moment due to tire lateral distortion (see ref. 1)

$$\phi = \left[1 + (L\nu_1)^2\right]^{-1/2}$$

ψ angle of rotation of wheel about swivel axis, radians

Subscript:

max maximum

HYSTERESIS FORCES AND MOMENTS FOR A STANDING TIRE

As a preliminary step for the analysis of tire hysteresis effects for a rolling tire, it is convenient to study first the hysteresis forces and moments acting on a standing tire subjected to cyclic lateral or torsional loading.

Lateral Hysteresis Force

Consider first the case of a standing tire the base of which is subjected to a periodical lateral deformation λ_0 of the form

$$\lambda_0 = \lambda_{0,max} \sin \nu t \qquad (1)$$

(where ν and t represent circular frequency and time, respectively) caused by an applied lateral ground force $F_{y,\lambda}$. (See sketch 1.) Under these conditions the lateral ground force is experimentally observed to vary with time in the manner indicated in sketch 2 so that the corresponding variation of lateral ground force with lateral tire deformation, shown in sketch 3, appears in the form of a

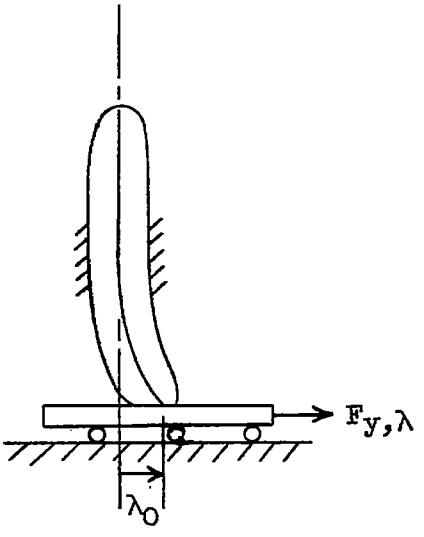

Sketch 1

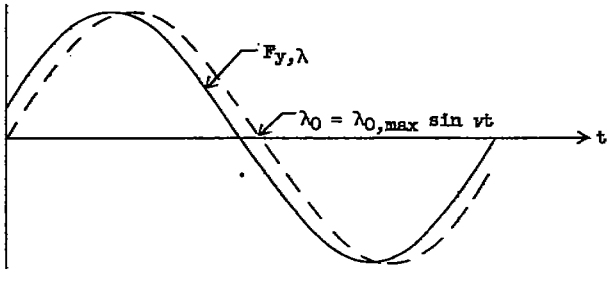

Sketch 2

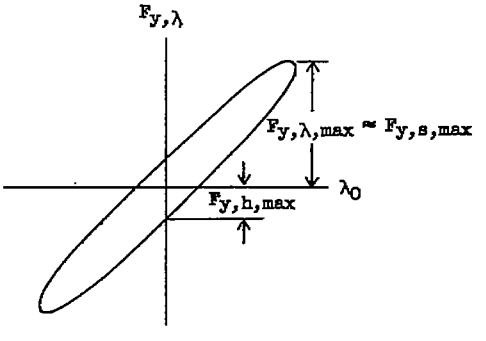

Sketch 3

typical hysteresis loop. This hysteresis loop arises largely as a consequence of the structural or hysteresis damping forces which oppose the tire deformation. (These forces are referred to hereinafter simply as hysteresis forces.) In the case of metallic structures it has been found that such hysteresis forces (1) appear to be independent of frequency, (2) have an amplitude usually equal to a small fraction of the amplitude of the corresponding spring forces, but shifted in phase by 90°, and (3) can be analytically represented with fair accuracy as the damping force generated by an equivalent viscous damper whose damping coefficient is inversely proportional to the frequency of oscillation. (See ref. 3, or any other book on aeroelasticity.) These same concepts are assumed to be applicable to the treatment of hysteresis effects in standing tires.

The lateral spring force $F_{y,s}$ in a tire for purely lateral oscillations is

$$F_{y,s} = K_\lambda \lambda_0 \tag{2}$$

where K_λ is the lateral spring constant. The corresponding hysteresis damping force, in accordance with the preceding assumptions, can be described by the equation

$$F_{y,h} = \frac{\eta_\lambda K_\lambda}{\nu} D_t \lambda_0 \tag{3}$$

where the parameter η_λ is the ratio of the maximum hysteresis force $F_{y,h,max}$ (see sketch 3) to the maximum spring force $F_{y,s,max}$, or, since the maximum total ground force $F_{y,\lambda,max}$ and the maximum spring force are approximately equal,

$$\eta_\lambda = \frac{F_{y,h,max}}{F_{y,\lambda,max}} \tag{4}$$

The total ground force $F_{y,\lambda}$ due to tire lateral distortion effects (exclusive of inertia effects, which are treated separately in ref. 1) can now be obtained by adding equations (2) and (3) to give

$$F_{y,\lambda} = K_\lambda \lambda_0 + \frac{\eta_\lambda K_\lambda}{\nu} D_t \lambda_0 \tag{5}$$

Before equation (5) can be used with confidence, it is necessary to investigate whether the hysteresis damping parameter η_λ is independent of frequency, as was assumed, and, if so, to determine its value. In this connection, some experimental hysteresis or damping-coefficient data are available from static force-deflection tests (partly published in refs. 4 and 5) and from dynamic free-vibration tests for lateral frequencies up to about 4 cycles per second (ref. 6). The static data are given in the references in the form of force-deflection hysteresis-loop plots similar to sketch 3 from which η_λ can be evaluated through use of equation (4). These data indicate that η_λ lies in the range $0.07 < \eta_\lambda < 0.18$. The dynamic free-vibration data are given in reference 6 in the form of plots of decrease in amplitude of the lateral oscillation per cycle. These data can be readily converted to give the corresponding values of η_λ by making use of the conversion equations of reference 3, which are also indicated in appendix B. The resulting values of η_λ lie in the range $0.08 < \eta_\lambda < 0.19$, which is about the same range as for the static data. Hence, the available experimental data roughly support the assumption that η_λ is independent of frequency (at least up to 4 cycles per second), or, in more general terms, these data support the assumption that the amplitudes of hysteresis forces are independent of the time rate of tire distortion.

Most of the aforementioned experimental data indicate that, to an accuracy of one significant figure,

$$\eta_\lambda = 0.1 \tag{6}$$

In view of the limited data, no attempt is made herein to define this quantity more precisely.

Hysteresis Moment

The preceding discussion of hysteresis effects associated with tire lateral stiffness obviously applies in an analogous manner to hysteresis effects associated with tire torsional stiffness. For example, the twisting-moment equations corresponding to equations (3) and (4) are

$$M_{z,h} = \frac{\eta_\alpha K_\alpha}{\nu} D_t\alpha \tag{7}$$

$$\eta_\alpha = \frac{M_{z,h,max}}{M_{z,\alpha,max}} \tag{8}$$

where

$M_{z,h}$	hysteresis twisting moment on tire due to twist of tire
α	twist in tire about a vertical axis, radians
K_α	torsional spring constant of standing tire
η_α	hysteresis-moment parameter analogous to η_λ for hysteresis force
$M_{z,h,max}$	maximum hysteresis moment
$M_{z,\alpha,max}$	maximum total twisting moment

In regard to the magnitude of the hysteresis-moment parameter η_α, little directly pertinent information is available. However, in order to obtain a rough estimate of η_α, it might be noted that the parameter η_λ for tire lateral distortion and the corresponding quantities η_x and η_z for tire fore-and-aft deformation and vertical deformation, respectively, are each approximately equal to each other and are all approximately equal to 0.1. (More precisely, the free-vibration data of ref. 6 indicate that $0.08 < \eta_\lambda < 0.19$, $0.10 < \eta_x < 0.15$, and $0.06 < \eta_z < 0.17$.) Then, since these η's are similarly defined as ratios of maximum hysteresis force to maximum total force and since the corresponding physical processes are similar, it is probably not too unrealistic to assume that η_α is of like magnitude or roughly

$$\eta_\alpha = 0.1 \tag{9}$$

As an additional check on the reliability of equation (9), several static moment hysteresis loops were available for a 44-inch-diameter

type III tire at its rated loading condition. These loops were taken at small twist angles to minimize tire skidding (which, according to the data of ref. 7, is usually important for twist angles greater than 1°); moreover, for this same purpose the ground-contact surface of the tire was glued to the ground surface (in this case a steel plate). These tests gave a value of η_α of 0.14 for a maximum twist angle of 1.5° and a value of 0.24 for an angle of 4°. These data indicate that the previously deduced rounded-off value of $\eta_\alpha = 0.1$ is probably realistic for very small angles but that it may be low for twist angles of several degrees or more.

In concluding this discussion of the hysteresis effects for a standing tire, it should be kept in mind that the equations derived in this section for hysteresis forces and moments contain the implication that the amplitudes of these forces and moments, for a given amplitude of tire distortion, are independent of frequency of distortion. This fact can be easily seen for the hysteresis force, for example, by inspection of the following equation obtained by substituting equation (1) into equation (3):

$$F_{y,h} = \eta_\lambda K_\lambda \lambda_{0,max} \cos \nu t \tag{10}$$

The corresponding amplitude of hysteresis force per unit of distortion $\frac{F_{y,h,max}}{\lambda_{0,max}} = \eta_\lambda K_\lambda$ is seen to be independent of velocity and frequency. This observation regarding distortion frequency is used in the next part of this paper as a basis for generalizing the just-derived force and moment equations to apply to the case of a rolling tire.

HYSTERESIS FORCES AND MOMENTS FOR A ROLLING TIRE

In this part of this paper equations are derived for the hysteresis forces and moments acting on a rolling tire.

Tire Deformation

This section summarizes the basic assumptions regarding tire lateral deformation during rolling which are utilized in the present analysis of hysteresis effects for a rolling tire. These assumptions and some justification for their adoption are discussed in more detail in reference 1.

The usual state of lateral deformation for a rolling tire is illustrated in figure 1, which shows two views of the tire - a side view and a bottom view taken perpendicular to the wheel axle. The primary factor of interest is the lateral distortion λ of the tire equator or peripheral center line. The actual shape of the equator curve is indicated by the dashed-line curve in the bottom view of figure 1. In the present analysis, this actual-shape curve is replaced by the solid-line assumed-shape curve. This assumed-shape curve consists of a straight-line segment for the ground-contact region and of two exponential-curve segments for the regions outside the ground-contact area.

For the ground-contact area (along the line 2-0-1 in fig. 1), the lateral distortion for the straight-line assumed-shape curve is described by the equation

$$\lambda = \lambda_0 + s\alpha \qquad (-h \leqq s \leqq h) \qquad (11)$$

where s is the circumferential coordinate on the tire.

Along the line 1-5-4 in figure 1, the lateral distortion is represented by the exponential equation

$$\lambda = \lambda_1 e^{-(s-h)/L} \qquad (h \leqq s \lessapprox \pi r) \qquad (12)$$

where h is the half-length of the ground-contact area, λ_1 is the lateral deformation of the tire equator at the foremost point of the ground-contact area, and L is a tire constant called the relaxation length. A physical interpretation of this relaxation length may be obtained by noting that it represents the circumferential distance s which must be traversed for the lateral distortion to drop to a fraction $1/e$ of its initial value, or that it represents the length of the normal projection on the wheel center plane of the line formed by extending a tangent to the exponential curve from the point 1 to the wheel center plane. (See fig. 1.)

Similarly, the tire-equator distortion off the rearmost edge of the ground-contact area is assumed to be given by the equation

$$\lambda = \lambda_2 e^{(s+h)/L} \qquad (h \leqq -s \lessapprox \pi r) \qquad (13)$$

(analogous to eq. (12)) where λ_2 is the lateral deformation at the rearmost point of the ground-contact area.

In regard to the accuracy of equations (12) and (13), it should be noted that the lateral-distortion curves of tires actually appear to obey exponential relations except possibly close to the leading and trailing edges of the ground-contact area. (See, for example, ref. 5.) Moreover, under normal rolling conditions, equation (12) is probably always fairly realistic even up to the leading edge of the ground-contact region. (See ref. 1.) However, equation (13) is not so accurate since it implies that a large sharp bend exists in the tire-equator curve at the rearmost ground-contact point 2. (See fig. 1.) In actuality, the tire cannot sustain such a sharp bend; therefore, the actual tire curve in this region is shaped more like the dashed-line curve for this region shown in figure 1 than like the solid-line assumed curve. Although this discrepancy is possibly of some importance in influencing the quantitative accuracy of the subsequent analysis, it will nevertheless be ignored in first approximation.

It should also be noted that, according to equation (11), the lateral deformations at the foremost and rearmost ground-contact points (λ_1 and λ_2, respectively) can be stated in the form

$$\lambda_1 = \lambda_0 + h\alpha \tag{14}$$

$$\lambda_2 = \lambda_0 - h\alpha \tag{15}$$

Equations (11) to (15) provide the basic equations of tire-equator distortion which are used for the subsequent analysis.

Also needed for the subsequent analysis are the time rates of change of tire lateral deformation for a given tire particle for regions 2-0-1, 1-5-4, and 2-6-4 in figure 1. These rates are obtained by differentiating equations (11), (12), and (13) with respect to time:

For region 2-0-1,

$$D_t\lambda = D_t\lambda_0 + sD_t\alpha + \alpha D_t s \tag{16}$$

for region 1-5-4,

$$D_t\lambda = e^{-(s-h)/L}\left(D_t\lambda_1 - \frac{\lambda_1}{L} D_t s\right) \tag{17}$$

and, for region 2-6-4,

$$D_t\lambda = e^{(s+h)/L}\left(D_t\lambda_2 + \frac{\lambda_2}{L} D_t s\right) \tag{18}$$

where D_t denotes the differential operator d/dt. The quantity $D_t s$, which is the peripheral velocity of tire-equator particles with respect to the wheel axle, is approximately equal to the negative of the rolling velocity v; hence, equations (16) to (18) may also be written as follows:

For region 2-0-1,

$$D_t\lambda = D_t\lambda_0 + sD_t\alpha - v\alpha \tag{19}$$

for region 1-5-4,

$$D_t\lambda = e^{-(s-h)/L}\left(D_t\lambda_1 + \frac{v}{L}\lambda_1\right) \tag{20}$$

and, for region 2-6-4,

$$D_t\lambda = e^{(s+h)/L}\left(D_t\lambda_2 - \frac{v}{L}\lambda_2\right) \tag{21}$$

Equations (19) to (21) provide the basic equations of rate of change of tire distortion which are used for the subsequent analysis.

Hysteresis Forces and Moments

Basic considerations.- In order to obtain an expression for the hysteresis forces and moments acting on a rolling tire, it is convenient to consider separately the three regions of the tire corresponding to equations (11) to (13) for tire-equator lateral deformation, that is, the regions 2-0-1, 1-5-4, and 2-6-4 indicated in figure 1. The resultant lateral hysteresis forces for these three regions are denoted, respectively, as F_0, F_1, and F_2. In each of these regions, the hysteresis forces

will obviously act in such a direction as to oppose relative motion or distortion of these regions. In other words, these hysteresis forces are qualitatively similar to the forces which would be generated by a series of linear viscous damper units located around the tire periphery, which laterally connect the tire equator with the rigid wheel, as indicated in the following sketch:

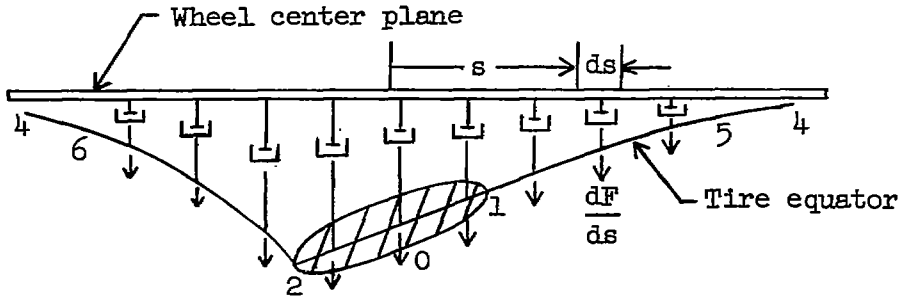

If this viscous-damper analogy is adopted, then the hysteresis force per unit circumferential distance (dF/ds) can be expressed by the equation for the damping force of a viscous damper as

$$\frac{dF}{ds} = kD_t\lambda \tag{22}$$

where k is the equivalent viscous damping coefficient of the tire per unit circumferential distance.

The total hysteresis force F_0 for the region 2-0-1 is obtained by inserting equation (19) for $D_t\lambda$ into equation (22) and integrating. Thus,

$$F_0 = \int_{s=-h}^{h} kD_t\lambda \, ds = k\int_{s=-h}^{h} (D_t\lambda_0 + sD_t\alpha - v\alpha)ds = 2hk(D_t\lambda_0 - v\alpha) \tag{23}$$

The total hysteresis force F_1 for the region 1-5-4 is obtained by inserting equation (20) for $D_t\lambda$ into equation (22). Thus,

$$F_1 = \int_{s=h}^{\approx \pi r} \frac{dF_1}{ds}\, ds = \int_{s=h}^{\approx \pi r} kD_t\lambda\, ds = \left[\int_{s=h}^{\approx \pi r} ke^{-(s-h)/L}\, ds\right]\left(D_t\lambda_1 + \frac{v}{L}\lambda_1\right) \tag{24}$$

Evaluation of the integral, after replacing the upper limit by infinity for simplification of the result (which introduces no significant error because of the rapidly decaying exponential function involved), yields the final expression

$$F_1 = Lk\left(D_t\lambda_1 + \frac{v}{L}\lambda_1\right) \tag{25}$$

Similarly, the following equation is obtained for the hysteresis force F_2 in the region 2-6-4 through the use of equations (21) and (22):

$$F_2 = \int_{-s=h}^{\approx \pi r} kD_t\lambda\, d(-s) = \left[\int_{(-s)=h}^{\approx \pi r} ke^{-(-s-h)/L}\, d(-s)\right]\left(D_t\lambda_2 - \frac{v}{L}\lambda_2\right) \tag{26}$$

which, after replacing the upper limit of integration by infinity and integrating, gives

$$F_2 = Lk\left(D_t\lambda_2 - \frac{v}{L}\lambda_2\right) \tag{27}$$

Sinusoidal motion.- In the present analysis, attention is restricted to problems where the tire-distortion parameters λ_1 and λ_2 vary sinusoidally with time at the circular frequency v. For such cases, λ_1 can be expressed as

$$\lambda_1 = \lambda_{1,max} \sin vt$$

Thus, equation (25) for the force F_1 in the region 1-5-4 can be expressed as

$$F_1 = Lk\lambda_{1,max}\left(\nu \cos \nu t + \frac{v}{L} \sin \nu t\right)$$

or

$$F_1 = Lk\lambda_{1,max}\sqrt{\nu^2 + \frac{v^2}{L^2}} \sin(\nu t + A)$$

where

$$A = \tan^{-1}(\nu L/v)$$

The corresponding amplitude of hysteresis force per unit amplitude of lateral distortion is then

$$\frac{F_{1,max}}{\lambda_{1,max}} = Lk\sqrt{\nu^2 + \frac{v^2}{L^2}} \tag{28}$$

From a similar consideration of the force F_2 in the region 2-6-4, the following equation is obtained:

$$\frac{F_{2,max}}{\lambda_{2,max}} = Lk\sqrt{\nu^2 + \frac{v^2}{L^2}} \tag{29}$$

During the earlier discussion of hysteresis effects on a standing tire, some evidence was offered to support the assumption that the amplitudes of lateral hysteresis forces in a tire for a given amplitude of lateral distortion are independent of the frequency of distortion. In order to apply this result to the rolling-tire case, it should first be recognized that the rate or effective frequency of distortion for the

individual particles in a rolling tire depends not only on shimmy frequency ν but also on the rolling velocity v. (For example, if the shimmy frequency approaches zero but the rolling velocity is finite, then the individual tire elements will obviously experience periodical lateral distortions at the frequency of rotation of the tire ($\approx v/r$).) Consequently, if hysteresis forces are independent of shimmy frequency for the rolling-tire case, as is suggested by the previously discussed data for the standing-tire case, then they are also necessarily independent of rolling velocity v. In view of this reasoning, the amplitude of the hysteresis force per unit amplitude of lateral distortion, which is equal to $Lk\sqrt{\nu^2 + \frac{v^2}{L^2}}$ according to both equations (28) and (29), is assumed hereinafter to be independent of both shimmy frequency and rolling velocity and, consequently, could be evaluated, for example, from tests of a standing tire. This quantity $Lk\sqrt{\nu^2 + \frac{v^2}{L^2}}$ will be abbreviated as K or, in other words,

$$k = \frac{K}{L\sqrt{\nu^2 + \frac{v^2}{L^2}}} \tag{30}$$

It should be kept in mind that K is independent of frequency and velocity.

Next consider the total lateral hysteresis force $F_{y,h} = F_0 + F_1 + F_2$. By use of equations (23), (25), (27), and (30), this force can be expressed in the form

$$F_{y,h} = \frac{K}{L\sqrt{\nu^2 + \frac{v^2}{L^2}}}\left[2h\left(D_t\lambda_0 - v\alpha\right) + L\left(D_t\lambda_1 + \frac{v}{L}\lambda_1\right) + L\left(D_t\lambda_2 - \frac{v}{L}\lambda_2\right)\right] \tag{31}$$

By substitution for λ_1 and λ_2 according to equations (14) and (15), equation (31) reduces to the following form:

$$F_{y,h} = \frac{2(L + h)K}{L\sqrt{\nu^2 + \frac{v^2}{L^2}}} D_t\lambda_0 \tag{32}$$

Next consider the hysteresis moments M_0, M_1, and M_2 about a vertical axis through the wheel center point, where M_0, M_1, and M_2 correspond to the regions 2-0-1, 1-5-4, and 2-6-4 in figure 1, respectively.

For the region 2-0-1 this moment is given by the equation

$$M_0 = \int_{s=-h}^{h} \frac{dF}{ds}\, s\, ds \tag{33}$$

and by use of equations (19), (22), and (30) this integral yields the result

$$M_0 = \int_{s=-h}^{h} kD_t\lambda s\, ds = k\int_{s=-h}^{h} \left(D_t\lambda_0 + sD_t\alpha - v\alpha\right)s\, ds = \frac{2}{3}h^3kD_t\alpha = \frac{2}{3}\frac{h^3K}{L\sqrt{\nu^2 + \frac{v^2}{L^2}}}D_t\alpha \tag{34}$$

The moments could also be obtained for the other two regions 1-5-4 and 2-6-4 by integrations similar to the integration for the region 2-0-1. However, for reasons to be discussed subsequently, the following approach for these moments is more convenient.

For the regions 1-5-4 and 2-6-4, the moments M_1 and M_2 can be expressed as the product of the corresponding forces F_1 and F_2 (see eqs. (25) and (27), respectively) and their center-of-pressure distances, j_1 and j_2 as

$$M_1 = F_1j_1 = Lkj_1\left(D_t\lambda_1 + \frac{v}{L}\lambda_1\right) \tag{35}$$

$$M_2 = -F_2 j_2 = -Ikj_2\left(D_t\lambda_2 - \frac{v}{L}\lambda_2\right) \tag{36}$$

Moreover, since the force per unit circumferential distance (dF/ds) has been taken to be linearly dependent on the lateral deformation λ (see eq. (22)) and since λ has the same shape of exponential variation with s for the two regions, the two center-of-pressure distances j_1 and j_2 evidently must be equal:

$$j_1 = j_2 \tag{37}$$

The total hysteresis twisting moment $M_{z,h}$ can now be obtained from the relation $M_{z,h} = M_0 + M_1 + M_2$ by use of equations (34) to (37) and (30) as

$$M_{z,h} = \frac{2}{3}\frac{h^3K}{L\sqrt{v^2 + \frac{v^2}{L^2}}}D_t\alpha + \frac{Kj_1}{\sqrt{v^2 + \frac{v^2}{L^2}}}\left[D_t\left(\lambda_1 - \lambda_2\right) + \left(\lambda_1 + \lambda_2\right)\frac{v}{L}\right]$$

or, after also applying equations (14) and (15), as

$$M_{z,h} = \frac{2K}{\sqrt{v^2 + \frac{v^2}{L^2}}}\left[\left(j_1 + \frac{h^2}{3L}\right)hD_t\alpha + \frac{j_1 v}{L}\lambda_0\right] \tag{38}$$

Equations (32) and (38) provide two equations for the hysteresis force and moment acting on a rolling (or standing) tire; however, these equations contain two as yet unevaluated parameters, namely, K and j_1. In order to express these parameters in terms of some measurable tire properties, these two equations may be compared with the previously derived equations for hysteresis force and moment on a standing tire. (See eqs. (3) and (7)). For a standing tire (v = 0), equations (32) and (38), respectively, reduce to the following relations:

$$F_{y,h} = \frac{2(L + h)K}{Lv} D_t \lambda_0 \tag{39}$$

$$M_{z,h} = \frac{2hK}{v}\left(j_1 + \frac{h^2}{3L}\right) D_t \alpha \tag{40}$$

Comparison of equations (3) and (39) yields the relation

$$K = \frac{L}{2(L + h)} \eta_\lambda K_\lambda \tag{41}$$

and comparison of equations (7) and (40), with the use of equation (41) to eliminate K, yields

$$j_1 = \frac{(L + h)\eta_\alpha K_\alpha}{Lh\eta_\lambda K_\lambda} - \frac{h^2}{3L} \tag{42}$$

In connection with the above determination of the center-of-pressure parameter j_1 in terms of the hysteresis parameter η_α, it might be recalled that it was not necessary to treat this quantity in the theory as an unknown parameter since j_1 could have been obtained directly by integration from the following equation:

$$j_1 = \frac{\int_{s=h}^{\approx \pi r} \frac{dF}{ds}\, j\, ds}{F_1} \tag{43}$$

where j is the moment arm of the incremental force dF. (See fig. 1.) However, only one unknown parameter would be involved in equations (32) and (38) if this procedure were followed, namely, K; consequently, no choice of this parameter K could in general satisfy both of the two end-point (zero-velocity) conditions prescribed by equations (3) and (7). For the present problem it was considered more realistic to satisfy both equations (3) and (7) rather than to satisfy only one of them together with equation (43).

After substitution of equation (41) into equation (32) and substitution of equations (41) and (42) into equation (38), the following equations result:

$$F_{y,h} = \frac{\eta_\lambda K_\lambda}{\sqrt{\nu^2 + \frac{v^2}{L^2}}} D_t \lambda_0 \tag{44}$$

$$M_{z,h} = \frac{\eta_\alpha K_\alpha}{\sqrt{\nu^2 + \frac{v^2}{L^2}}} \left(D_t \alpha + \zeta \frac{v}{hL} \lambda_0 \right) \tag{45}$$

where

$$\zeta = 1 - \frac{\eta_\lambda K_\lambda h^3}{3(L + h)\eta_\alpha K_\alpha} \tag{46}$$

Finally, by use of the relations

$$D_t \equiv \frac{d}{dt} = \frac{dx}{dt} \frac{d}{dx} = v \frac{d}{dx} \equiv vD \tag{47}$$

$$\nu_1 = \frac{\nu}{v} \tag{48}$$

where ν_1 is called the path frequency, equations (44) and (45) can be expressed in the following convenient forms:

$$\left.\begin{aligned} F_{y,h} &= \frac{\eta_\lambda K_\lambda}{\sqrt{1 + (L\nu/v)^2}} \frac{L}{v} D_t\lambda_0 \\ F_{y,h} &= \frac{\eta_\lambda K_\lambda L}{\sqrt{1 + (L\nu_1)^2}} D\lambda_0 \end{aligned}\right\} \tag{49}$$

$$\left.\begin{aligned} M_{z,h} &= \frac{\eta_\alpha K_\alpha}{\sqrt{1 + (L\nu/v)^2}}\left(\frac{L}{v} D_t\alpha + \frac{\zeta}{h}\lambda_0\right) \\ M_{z,h} &= \frac{\eta_\alpha K_\alpha}{\sqrt{1 + (L\nu_1)^2}}\left(LD\alpha + \frac{\zeta}{h}\lambda_0\right) \end{aligned}\right\} \tag{50}$$

Equations (49) and (50) are the final equations for the hysteresis force and moment acting on a rolling tire the base of which is experiencing a sinusoidal disturbance at some circular frequency ν.

IMPORTANCE OF HYSTERESIS EFFECTS

In order to assess the importance of the hysteresis force and moment terms given by equations (49) and (50), these equations are now applied to two simple cases of wheel motion. One case is for general shimmying motion at large shimmy wavelengths (including the limiting condition of steady yawed rolling) and the other case is for wheel shimmy where the wheel has only one degree of freedom, namely, rotation about an inclined swivel axis.

Large-Wavelength Rolling

Theoretical considerations.- Consider first the special case of an untilted wheel rolling in such a manner that the wavelength of any lateral or torsional oscillation ($S = 2\pi v/\nu$) is extremely large in comparison with the tire characteristic dimensions (for example, L and h). These conditions are satisfied for some high-speed rolling cases and for the special case of steady yawed rolling; they are not satisfied for some medium-speed cases and are rarely satisfied for very-low-speed shimmy oscillations.

For the conditions just mentioned, the ratio $L\nu/v$ becomes negligible; hence, this ratio, the quantity $\frac{L}{v} D_t\lambda_O$ (whose amplitude is equal to $\frac{L\nu}{v} \lambda_{O,max}$ for sinusoidal oscillations), and the quantity $\frac{L}{v} D_t\alpha$ can be set equal to zero in equations (49) and (50). Also, the following equation, relating tire lateral deformation and twist for these conditions, is valid (see approximation C2 of ref. 1):

$$\lambda_O = -l_1\alpha \tag{51}$$

where

$$l_1 = L + h \tag{52}$$

Application of these simplifications to equations (49) and (50) yields

$$F_{y,h} = 0 \tag{53}$$

$$M_{z,h} = \zeta\eta_\alpha K_\alpha \frac{l}{h} \lambda_O = -\zeta\eta_\alpha K_\alpha \frac{l_1}{h} \alpha \tag{54}$$

Equation (53) indicates that, to a first approximation, the net resultant lateral hysteresis force, for the considered rolling conditions, is zero. (The incremental internal hysteresis forces are, of course, still as large as for any other rolling condition, but since some of them act in opposite directions, it is possible for the resultant force to become zero.)

The hysteresis moment, according to equation (54), is, however, finite. In order to appreciate better the quantitative importance of this moment, it is convenient to consider the total spring and hysteresis moment acting on the tire. This total moment $M_{z,\alpha}$ is the sum of the elastic moment $M_{z,s}$, where

$$M_{z,s} = K_\alpha \alpha \tag{55}$$

and of the hysteresis moment (eq. (54)); that is,

$$M_{z,\alpha} = M_{z,s} + M_{z,h} = K_\alpha \alpha - \zeta \eta_\alpha K_\alpha \frac{l_1}{h} \alpha = \left(1 - \zeta \eta_\alpha \frac{l_1}{h}\right) K_\alpha \alpha \tag{56}$$

It can be readily seen from the final form of equation (56) that the essential action of the hysteresis moment is to reduce effectively the torsional spring constant for a rolling tire $\left(\text{defined as } K_{\alpha,r} = M_{z,\alpha}/\alpha\right)$ below the corresponding static spring constant K_α by the factor $\left(1 - \zeta \eta_\alpha \frac{l_1}{h}\right)$; that is,

$$K_{\alpha,r} = \left(1 - \zeta \eta_\alpha \frac{l_1}{h}\right) K_\alpha \tag{57}$$

With the aid of equation (57), the present hysteresis analysis can now be partly assessed both by examining the magnitude of the calculated hysteresis effects and by comparing calculated results with corresponding experimental data.

In regard to the magnitude of the effective reduction of torsional stiffness, for some possible sizes of tire constants, equation (57) gives an effective stiffness reduction of as much as 28 percent (see subsequent calculations) if η_α is taken as 0.1. (If η_α is taken as 0.2, this percentage is approximately doubled.) Thus, it appears that hysteresis effects may be of some importance for analyzing the rolling behavior of tires, at least for conditions where tire torsional stiffness is involved.

Comparison with experiment.- Some rough experimental confirmation of the present theory can be obtained by comparison of the predictions of equation (57) with the experimental data of references 8 and 5 for the case of steady yawed rolling in a straight-line path.

Experimental data from reference 8 for a 10-inch-diameter tail-wheel tire, together with the corresponding theoretical calculation according to equation (57) (with η_λ and η_α taken as 0.1), are as follows:

L, cm	10
h, cm	5.2
K_λ, kg/cm	45
K_α, kg-cm/radian	3,040
$K_{\alpha,r}$, kg-cm/radian:	
Experimental	2,270
Calculated (eq. (57))	2,190

Fair agreement is indicated between calculated and experimental values of rolling torsional stiffness $K_{\alpha,r}$.

A similar comparison for a pair of current 26-inch-diameter, 26 × 6.6, 12-ply-rating, type VII aircraft tires, based on data from reference 5 (for a vertical tire deflection of 2 inches and an inflation pressure of 142 pounds per square inch) with η_λ and η_α taken as 0.1, is given as follows:

L, in.	5 to 9
h, in.	6.1
K_λ, lb/in.	1,950
K_α, lb-in./deg	1,420
$K_{\alpha,r}$, lb-in./deg:	
Experimental	1,050
Calculated (eq. (57))	1,180 to 1,090

In spite of the large amount of doubt regarding the magnitude of the relaxation length L for these latter data, the agreement between the experimental and calculated values of $K_{\alpha,r}$ is still seen to be good enough to furnish at least a rough confirmation of the present theory.

Wheel Shimmy

A second indication of the effects of hysteresis may be obtained by considering the problem of shimmy for an idealized landing gear the wheel of which has only one degree of freedom, aside from coupled lateral and torsional tire distortion, namely, rotation about an inclined swivel axis. (See fig. 2.) The equations of motion and conditions for stable motion for this simplified case are derived in appendix A according to

the summary theory of reference 1, as modified to take into account the effects of hysteresis on the lateral force and twisting moment as given by equations (49) and (50). The final equations for the stability conditions correlating landing-gear trail a, rolling velocity v, and minimum viscous shimmy damper constant g (damper moment $gD_t\psi$) required for stable motion are given by equations (A22) to (A24) of appendix A. In addition, the corresponding stability-boundary conditions for a simplified version of the summary theory, designated as approximation B in reference 1, are given by equations (A22), (A24), and (A26).

Comparisons with experiment.- For this case, experimental stability-boundary and shimmy-frequency data for a small model landing gear (10-inch-diameter tire) are available in references 2 and 9 and are reproduced in figures 3 and 4 together with the corresponding predictions of the summary theory and approximation B to the summary theory, both with and without consideration of hysteresis effects. (The tire constants used for these calculations, as taken from refs. 2 and 8, are listed in appendix C.[1]) In regard to the significance of approximation B, it might be noted that this simplified version of the summary theory is almost the same as the more advanced of the two theories proposed by Bourcier de Carbon in reference 10.

By comparison of the theoretical curves in figures 3 and 4 with the corresponding experimental data it is seen that, for both the summary theory and approximation B, the theoretical curves with hysteresis considered are much closer to the experimental data than the theoretical curves with hysteresis not considered, both in regard to shape of curves and quantitative agreement with experiment. Hence, these experimental data appear to substantiate partly the reliability of the present analysis of hysteresis effects.

It might also be noted that approximation B appears to give better agreement with experiment than the summary theory to which it is an approximation. This result is probably a coincidence; in any event, it is of little significance since the differences between these two theories for these test conditions correspond to small high-order terms in the summary theory and there is little reason to believe that these high-order terms are described sufficiently accurately by the summary theory to insure that it is any more accurate than approximation B.

---

[1]It might be noted that the theoretical curves of figures 3 and 4 for the condition with hysteresis not considered differ slightly from the corresponding theoretical curves in reference 1. This difference results from the fact that the present theoretical curves were based on the experimentally determined value of footprint length whereas the curves of reference 1 were based on an effective value of footprint length which was indirectly calculated from the cornering power of the tire.

Sample calculations of damping required for stability.- As a final point of possible interest, some theoretical calculations were made of the minimum damping required to stabilize the motion of a hypothetical landing gear having the relative dimensions and properties $L = 0.8r$, $h = 0.5r$, $K_\alpha = 0.52r^2K_\lambda$, $\kappa = 0$, and $\tau = 0.1I_\psi/r^2$ for the following two values of trail: $a = 0.5r$ and $a = 0$. The required minimum damping, calculated according to approximation B (see eqs. (A22), (A24), and (A26)), is shown as a function of rolling velocity in figure 5. Three types of calculations are shown in this figure. The solid-line curves represent solutions with complete neglect of hysteresis effects $(\eta_\lambda = \eta_\alpha = 0)$. The short-dashed-line curves represent solutions with hysteresis effects included in detail $(\eta_\lambda = \eta_\alpha = 0.1)$. The third set of curves (short-dash—long-dash), designated as approximate hysteresis solution, represents solutions made under the assumption that the wavelength of the shimmy motion is large enough to allow the general hysteresis force and moment equations (49) and (50) to be replaced by the simpler equations (53) and (54).

Comparison of the solid- and dashed-line curves in figure 5 indicates that the hysteresis effects act in such a manner that the damping required to stabilize the landing-gear motion is appreciably reduced, and especially so at very low speeds and for the small-trail (zero) case. The maximum damping requirement is seen to be reduced by about 40 percent for the zero-trail condition and 20 percent for the large-trail ($a = 0.5r$) condition.

By examination of the curves in figure 5 for the approximate hysteresis solution, the approximate hysteresis solution is seen to give results which usually lie somewhere between the solution with hysteresis effects included in detail and the solution with hysteresis effects completely neglected. This fact indicates that taking the hysteresis effects into account by the approximate method is better than not taking them into account at all. This last point is of some importance for application of the present hysteresis theory to complex landing-gear configurations inasmuch as the detailed hysteresis solution might present some mathematical difficulties, whereas the approximate solution never involves any more work than the solution which completely neglects hysteresis effects.

Even though the approximate hysteresis solutions in figure 5 are better than solutions with no consideration of hysteresis effects at all, they are seen to be completely inadequate to represent the detailed hysteresis solution at low speeds, particularly for the small-trail condition. Moreover, not even for the highest speed condition shown do the two solutions coincide completely; thus, at least for this particular landing-gear configuration, the high-speed range where the approximate hysteresis solution might be expected to be valid either lies beyond the speed range of practical interest (that is, the range where positive damping is required) or does not exist at all.

CONCLUDING REMARKS

This paper has presented an approximate theoretical analysis of the hysteresis forces and moments acting on a rolling tire and has shown some limited experimental confirmation of the results of the analysis. Although this analysis cannot be said to give an extremely accurate answer to the tire-hysteresis problem, it is believed that the essential features of the hysteresis phenomena have been considered in a more realistic manner than in previous analyses.

Langley Aeronautical Laboratory,
National Advisory Committee for Aeronautics,
Langley Field, Va., February 21, 1957.

APPENDIX A

EQUATIONS OF MOTION AND STABILITY CONDITIONS FOR A SIMPLE CASE OF WHEEL SHIMMY

This appendix presents a derivation of the equations of motion for one of the simplest cases of wheel shimmy, where the rolling wheel has only one degree of freedom aside from tire distortion, namely, rotation about an inclined swivel axis by an angle ψ. (See fig. 2.) The rotation of the wheel about the swivel axis is assumed to be opposed by a linear torsion spring of moment $\rho\psi$ and a viscous shimmy damper of moment $gD_t\psi$. This derivation is made by modifying the pertinent equations for the summary theory of reference 1 to take into account the hysteresis force and moment according to equations (49) and (50).

Derivation of Equations of Motion

The important geometric parameters involved for this case, which is the same as case I in reference 1, are illustrated in figure 2. They include the wheel trail a, the angle of rotation about the swivel axis ψ, the swivel-axis inclination angle κ, the angle of rotation of the wheel about a vertical Z-axis θ, the tire-twist angle α, the lateral deflection of the tire equator from the XZ-plane at the center of the ground-contact area y_0, and the lateral ground deflection of the wheel $\eta_0 = y_0 - \lambda_0$ (lateral distance between XZ-plane of undisturbed motion and intersection of wheel center plane and ground plane below wheel axle).

First consider the moment M_h of the ground force about the swivel axis due to hysteresis effects (see fig. 2):

$$M_h = M_{z,h} \cos \kappa - aF_{y,h} \tag{A1}$$

where $F_{y,h}$ and $M_{z,h}$ are given by equations (49) and (50). A more convenient form of equation (A1) can be obtained by making use of the following geometric relations:

$$\theta = \psi \cos \kappa \tag{A2}$$

$$\eta_0 = -a\psi \tag{A3}$$

$$\lambda_0 = y_0 - \eta_0 = y_0 + a\psi \tag{A4}$$

$$\alpha = Dy_0 - \theta = Dy_0 - \psi \cos \kappa \tag{A5}$$

(Eq. (A5)) implies no skidding between tire and ground.) Substitution of equations (49) and (50) into equation (A1) and then substitution of equations (A4) and (A5) into this equation gives

$$M_h = \frac{1}{\sqrt{1 + (L\nu_1)^2}}\left(\eta_\alpha K_\alpha LD\alpha \cos \kappa - \eta_\lambda K_\lambda LaD\lambda_0 + \frac{\zeta \eta_\alpha K_\alpha}{h} \lambda_0 \cos \kappa\right)$$

$$= \frac{1}{\sqrt{1 + (L\nu_1)^2}}\left[\eta_\alpha K_\alpha LD^2 y_0 \cos \kappa - \eta_\lambda K_\lambda LaDy_0 + \frac{\zeta \eta_\alpha K_\alpha}{h} y_0 \cos \kappa - \right.$$

$$\left.\left(\eta_\alpha K_\alpha \cos^2 \kappa + \eta_\lambda K_\lambda a^2\right) LD\psi + \frac{\zeta a \eta_\alpha K_\alpha}{h} \psi \cos \kappa\right] \tag{A6}$$

which expresses the hysteresis moment as a function of y_0 and ψ.

Other moments acting about the swivel axis are the spring moments due to tire lateral distortion and twist, the moment of the vertical ground force F_z due to wheel swiveling and tilting and to tire lateral deformation, the moment due to tire-distortion gyroscopic effects, the spring restoring and viscous damper moments, and the inertia-reaction moment $\left(I_\psi D_t^2 \psi\right)$. (See ref. 1 for a discussion of these various moments.)

The sum of these other moments, in a form convenient for present use, is set equal to zero in equation (115a) of reference 1. In order to modify this equation to include the present hysteresis terms, it is necessary only to subtract the term M_h, as given by equation (A6), from the left-hand side of equation (115a) of reference 1. This procedure gives

$$G_1 D^2 \psi + G_2 D\psi + G_3 \psi + H_1 D^2 y_0 + H_2 Dy_0 + H_3 y_0 = 0 \tag{A7}$$

where

$$\left.\begin{aligned} G_1 &= I_\psi v^2 \\ G_2 &= a\tau v^2 \cos\kappa + gv + \phi L\left(\eta_\alpha K_\alpha \cos^2\kappa + \eta_\lambda K_\lambda a^2\right) \\ G_3 &= a^2 K_\lambda + K_\alpha \cos^2\kappa + \rho + \rho_\kappa - \frac{\phi\zeta a \eta_\alpha K_\alpha}{h}\cos\kappa \\ H_1 &= -\phi\eta_\alpha K_\alpha L \cos\kappa \\ H_2 &= -K_\alpha \cos\kappa + \tau v^2 \cos\kappa + \phi\eta_\lambda K_\lambda L a \\ H_3 &= aK_\lambda + c_\lambda F_z \sin\kappa - \frac{\phi\zeta\eta_\alpha K_\alpha}{h}\cos\kappa \end{aligned}\right\} \tag{A7a}$$

$$\phi = \frac{1}{\sqrt{1 + \left(L\nu_1\right)^2}} \tag{A8}$$

$$\rho_\kappa = \left(aK_\gamma - aF_z + ac_\lambda F_z + c_\gamma F_z \sin\kappa\right)\sin\kappa \tag{A9}$$

where I_ψ is the moment of inertia of the wheel structure about the swivel axis, F_z is the vertical ground force, c_λ is the lateral shift of vertical-force center of pressure per unit of lateral tire distortion, c_γ is the lateral shift of vertical-force center of pressure per radian of wheel lateral tilt, K_γ is the lateral elastic force per radian of lateral wheel tilt, and τ is a tire parameter associated with gyroscopic moments due to tire lateral distortion. (See eqs. (33) and (50) of ref. 1 for definitions of τ.)

Equation (A7) gives one relation between wheel rotation ψ and lateral deflection of the ground-contact area y_0. A second equation relating these two variables is furnished by the following kinematic equation (117) of reference 1:

$$\left(\sigma l_1 \cos \kappa - a\right)\psi - \sum_{n=0}^{\infty} l_n D^n y_0 = 0 \tag{A10}$$

where

$$l_n = \frac{(nL + h)h^{n-1}}{n!} \tag{A11}$$

$$\sigma = 1 + \frac{\xi L h}{r l_1} \tan \kappa \tag{A12}$$

where r is the tire radius and ξ is a number associated with tire tilt (see ref. 1) which is smaller than unity and probably close to zero.

Equations (A7) and (A10) are the basic equations of motion for the present case of shimmy with one degree of wheel freedom, according to the summary theory of reference 1, as modified to include the present hysteresis effects.

Conditions for Stable Motion

Among the most important characteristics of the wheel motion corresponding to equations (A7) and (A10) are the conditions governing steady-state motion of the wheel and the minimum damping required for stable motion. These conditions are found by the usual procedure of assuming that the two variables ψ and y_0 are purely oscillatory functions of distance rolled according to relations of the form

$$\psi = \psi_{max} e^{i\nu_1 x} \tag{A13}$$

$$y_0 = y_{0,max} e^{i\left(\nu_1 x + q\right)} \tag{A14}$$

where ψ_{max}, $y_{0,max}$, and q are constants.

Substitution of equations (A13) and (A14) into equations (A7) and (A10), division by $e^{i\nu_1 x}$, and separation of real and imaginary parts of each resulting equation provides the following four relations:

From equation (A7),

$$\left(G_3 - G_1\nu_1^2\right)\psi_{max} + \left(H_3 - H_1\nu_1^2\right)\left(y_{0,max}\cos q\right) - H_2\nu_1\left(y_{0,max}\sin q\right) = 0 \tag{A15}$$

$$G_2\nu_1\psi_{max} + H_2\nu_1\left(y_{0,max}\cos q\right) + \left(H_3 - H_1\nu_1^2\right)\left(y_{0,max}\sin q\right) = 0 \tag{A16}$$

and, from equation (A10),

$$\left(\sigma l_1\cos\kappa - a\right)\psi_{max} - p_{1\infty}\left(y_{0,max}\cos q\right) + p_{2\infty}\left(y_{0,max}\sin q\right) = 0 \tag{A17}$$

$$p_{2\infty}\left(y_{0,max}\cos q\right) + p_{1\infty}\left(y_{0,max}\sin q\right) = 0 \tag{A18}$$

where (see eqs. (80) of ref. 1)

$$\left.\begin{aligned} p_{1\infty} &= 1 - l_2\nu_1^2 + l_4\nu_1^4 - \cdots \\ &= \cos\nu_1 h - L\nu_1\sin\nu_1 h \\ p_{2\infty} &= l_1\nu_1 - l_3\nu_1^3 + l_5\nu_1^5 - \cdots \\ &= \sin\nu_1 h + L\nu_1\cos\nu_1 h \end{aligned}\right\} \tag{A19}$$

For nonzero values of the three quantities ψ_{max}, $\left(y_{0,max}\cos q\right)$, and $\left(y_{0,max}\sin q\right)$, the determinants of their coefficients must vanish for each group of three of the four equations (A15) to (A18). For example, from equations (A15), (A17), and (A18),

$$\begin{vmatrix} G_3 - G_1\nu_1^2 & H_3 - H_1\nu_1^2 & -H_2\nu_1 \\ \sigma l_1 \cos \kappa - a & -p_{1\infty} & p_{2\infty} \\ 0 & p_{2\infty} & p_{1\infty} \end{vmatrix} = 0 \tag{A20}$$

and, from equations (A16), (A17), and (A18),

$$\begin{vmatrix} G_2\nu_1 & H_2\nu_1 & H_3 - H_1\nu_1^2 \\ \sigma l_1 \cos \kappa - a & -p_{1\infty} & p_{2\infty} \\ 0 & p_{2\infty} & p_{1\infty} \end{vmatrix} = 0 \tag{A21}$$

Equations (A20) and (A21) can be expressed in a more convenient form by multiplying out the two determinants and substituting the values for the coefficients G and H from equation (A7a). Then, solving the resulting form of equation (A20) for v gives

$$v^2 = \frac{\left(a^2K_\lambda + K_\perp \cos^2\kappa + \rho + \rho_\kappa - \frac{\beta\zeta a\eta_\perp K_\perp}{h}\cos\kappa\right)\left(p_1^2 + p_2^2\right) + \left[\left(aK_\lambda + c_\lambda F_z \sin\kappa - \frac{\beta\zeta\eta_\perp K_\perp}{h}\cos\kappa + \beta\nu_1^2\eta_\perp K_\perp L\cos\kappa\right)p_1 - \left(K_\perp \cos\kappa - \beta\eta_\lambda K_\lambda I a\right)\nu_1 p_2\right]\left(\sigma l_1\cos\kappa - a\right)}{I_\psi\nu_1^2\left(p_1^2 + p_2^2\right) - \tau\nu_1 p_2\left(\sigma l_1\cos\kappa - a\right)\cos\kappa} \tag{A22}$$

where, for the summary theory,

$$\left.\begin{aligned} p_1 = p_{1\infty} &= \cos\ \nu_1 h - L\nu_1\ \sin\ \nu_1 h \\ p_2 = p_{2\infty} &= \sin\ \nu_1 h + L\nu_1\ \cos\ \nu_1 h \end{aligned}\right\} \tag{A23}$$

and solving the resulting form of equation (A21) for g gives

$$g = \frac{\left(\sigma l_1\cos\kappa - a\right)\left[\left(aK_\lambda + c_\lambda F_z \sin\kappa - \frac{\beta\zeta\eta_\perp K_\perp}{h}\cos\kappa + \beta\nu_1^2\eta_\perp K_\perp L\cos\kappa\right)p_2 + \nu_1 p_1\left(K_\perp\cos\kappa - \tau\nu^2\cos\kappa - \beta\eta_\lambda K_\lambda I a\right)\right]}{\nu_1\tau\left(p_1^2 + p_2^2\right)} - a\tau\nu\cos\kappa - \left(\eta_\perp K_\perp\cos^2\kappa + \eta_\lambda K_\lambda a^2\right)\beta\zeta\frac{I_\psi}{\tau} \tag{A24}$$

Equation (A22) gives the rolling velocity v as a function of shimmy path frequency ν_1, and equation (A24) furnishes the required minimum damping constant g for stable motion as a function of velocity and path frequency.

The preceding equations (A22) to (A24) give the characteristics of the wheel motion corresponding to the modified summary theory of reference 1. The corresponding equations for two simplified versions of this summary theory (approximations A and B of ref. 1) are obtained by replacing equations (A23) by the following equations:

For approximation A,

$$\left.\begin{aligned} p_1 &= 1 - l_2\nu_1^2 \\ p_2 &= l_1\nu_1 - l_3\nu_1^3 \end{aligned}\right\} \tag{A25}$$

and, for approximation B,

$$\left.\begin{aligned} p_1 &= 1 - l_2\nu_1^2 \\ p_2 &= l_1\nu_1 \end{aligned}\right\} \tag{A26}$$

Although other even more simplified versions of the summary theory are possible (see approximations C1, C2, D1, D2, and D3 of ref. 1), these other versions are too crude to be of much value for low-speed shimmy conditions, which are the conditions where hysteresis effects would be expected to be most important.

APPENDIX B

DETERMINATION OF HYSTERESIS CONSTANTS FROM FREE-VIBRATION TESTS

This appendix discusses a procedure for determining the lateral-hysteresis-force parameter η_λ (see eq. (4)) from information gained by free-vibration tests of a two-wheel cart of the type described in reference 6. Such a cart can be approximately represented by the linear mass-spring-damper system illustrated in the following sketch:

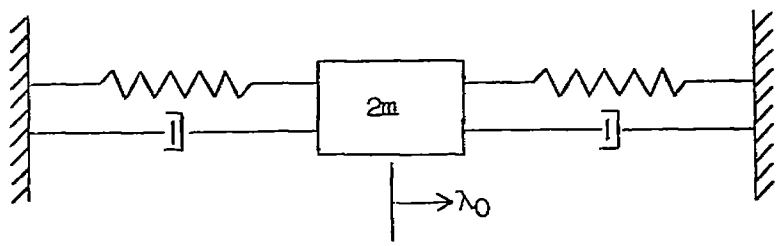

where the springs represent the two tire stiffnesses, the dampers represent the hysteresis damping, and $2m$ represents the mass of the cart. The spring and damping forces are given by equations (2) and (3) and the corresponding differential equation for the system for free oscillations is

$$2mD_t^2\lambda_0 + 2\frac{\eta_\lambda K_\lambda}{\nu} D_t\lambda_0 + 2K_\lambda\lambda_0 = 0$$

The solution of this equation is of the form

$$\lambda_0 = \varphi_1 e^{-\frac{\eta_\lambda K_\lambda}{2\nu m}t} \sin\left(\nu t + \varphi_2\right) \tag{B1}$$

where φ_1 and φ_2 are constants and

$$\nu = \sqrt{\frac{K_\lambda}{m} - \left(\frac{\eta_\lambda K_\lambda}{2\nu m}\right)^2} = \sqrt{\frac{K_\lambda}{m}\left(1 - \frac{\eta_\lambda^2 K_\lambda}{4m\nu^2}\right)} \tag{B2}$$

Inasmuch as $\frac{\eta_\lambda^2 K_\lambda}{4m\nu^2} \ll 1$ for conventional tires, equation (B2) can almost always be replaced by the simpler expression

$$\nu = \sqrt{\frac{K_\lambda}{m}} \tag{B3}$$

and, thus, equation (B1) can be reduced to the form

$$\lambda_0 = \varphi_1 e^{-\frac{1}{2}\eta_\lambda \nu t} \sin\left(\nu t + \varphi_2\right) \tag{B4}$$

The decrease in amplitude of the lateral oscillation per cycle $\left(\text{of period } T = \frac{1}{f} = \frac{2\pi}{\nu}\right)$ is then

$$\frac{\lambda_0(t + T)}{\lambda_0(t)} = e^{-\frac{1}{2}\eta_\lambda \nu T} = e^{-\pi\eta_\lambda} \tag{B5}$$

Since this ratio can be directly measured in free-vibration tests, equation (B5) provides the necessary relation for determining the parameter η_λ from such test data. Also equation (B3) gives the necessary equation for determining the lateral spring constant in terms of the experimental frequency and the cart mass.

APPENDIX C

CONSTANTS FOR CALCULATIONS

Most of the tire constants used for the calculations in figures 3 and 4 were obtained from references 2 and 8 and are as follows:

$$\kappa = \rho = g = 0$$

$$h = 5.2 \text{ cm}$$

$$L = 10 \text{ cm}$$

$$l_1 = L + h = 15.2 \text{ cm}$$

$$K_\lambda = 45 \text{ kg/cm}$$

$$K_\alpha = 3{,}040 \text{ cm-kg/radian}$$

$$I_\psi \approx 0.53 + 0.0025a^2 \text{ cm-kg-sec}^2$$

Both η_λ and η_α were taken equal to 0.1. In addition to these relations, the parameter τ, representing a gyroscopic moment due to tire lateral distortion (see ref. 1), was assumed to be equal to zero. Although a rough value of τ could perhaps have been estimated, such an estimate did not appear necessary because the effect of this parameter, according to any reasonable estimate of τ, would be of little importance in the velocity range of the experimental data in figures 3 and 4.

REFERENCES

1. Smiley, Robert F.: Correlation, Evaluation, and Extension of Linearized Theories for Tire Motion and Wheel Shimmy. NACA TN 3632, 1956.

2. Von Schlippe, B., and Dietrich, R.: Das Flattern eines mit Luftreifen versehenen Rades. (Flutter of a Wheel With Pneumatic Tire.) Tech. Berichte der Z.W.B., Bd. 11, Heft 2, 1944. (Available in English translation from ASTIA as ATI 51760.)

3. Scanlan, Robert H., and Rosenbaum, Robert: Introduction to the Study of Aircraft Vibration and Flutter. The Macmillan Co., 1951.

4. Horne, Walter B.: Static Force-Deflection Characteristics of Six Aircraft Tires Under Combined Loading. NACA TN 2926, 1953.

5. Horne, Walter B., Smiley, Robert F., and Stephenson, Bertrand H.: Low-Speed Yawed-Rolling Characteristics and Other Elastic Properties of a Pair of 26-Inch-Diameter, 12-Ply-Rating, Type VII Aircraft Tires. NACA TN 3604, 1956.

6. Horvay, G., and Crowe, R. E.: Spring and Damping Constants of Helicopter Tires. Eng. Rep. No. H-122-1 (Contract NO a(s)-3703), Helicopter Res. Div., McDonnell Aircraft Corp., July 17, 1945.

7. Boeckh: Ermittlung der elastischen Konstanten von Flugzeugreifen. (Determination of the Elastic Constants of Airplane Tires.) Focke-Wulf Flugzeugbau GmbH (Bremen), Dec. 1944. (Available in English translation as NACA TM 1378, 1954.)

8. Von Schlippe, B., and Dietrich, R.: Zur Mechanik des Luftreifens. (The Mechanics of Pneumatic Tires.) Junkers Flugzeug- und Motorenwerke, A.-G. (Dessau). (Translation available from ASTIA as ATI 105296.)

9. Von Schlippe, B., and Dietrich, R.: Das Flattern eines bepneuten Rades. (Shimmying of a Pneumatic Wheel.) Bericht 140, L.G.L., 1941, pp. 35-45, 63-66. (Available in English translation as NACA TM 1365, 1954, pp. 125-160, 217-228.)

10. Bourcier de Carbon, Christian: Étude Théorique du Shimmy des Roues d'Avion. (Analytical Study of Shimmy of Airplane Wheels.) Office National d'Études et de Recherches Aéronautiques, Publication No. 7, 1948. (Available in English translation as NACA TM 1337, 1952.)

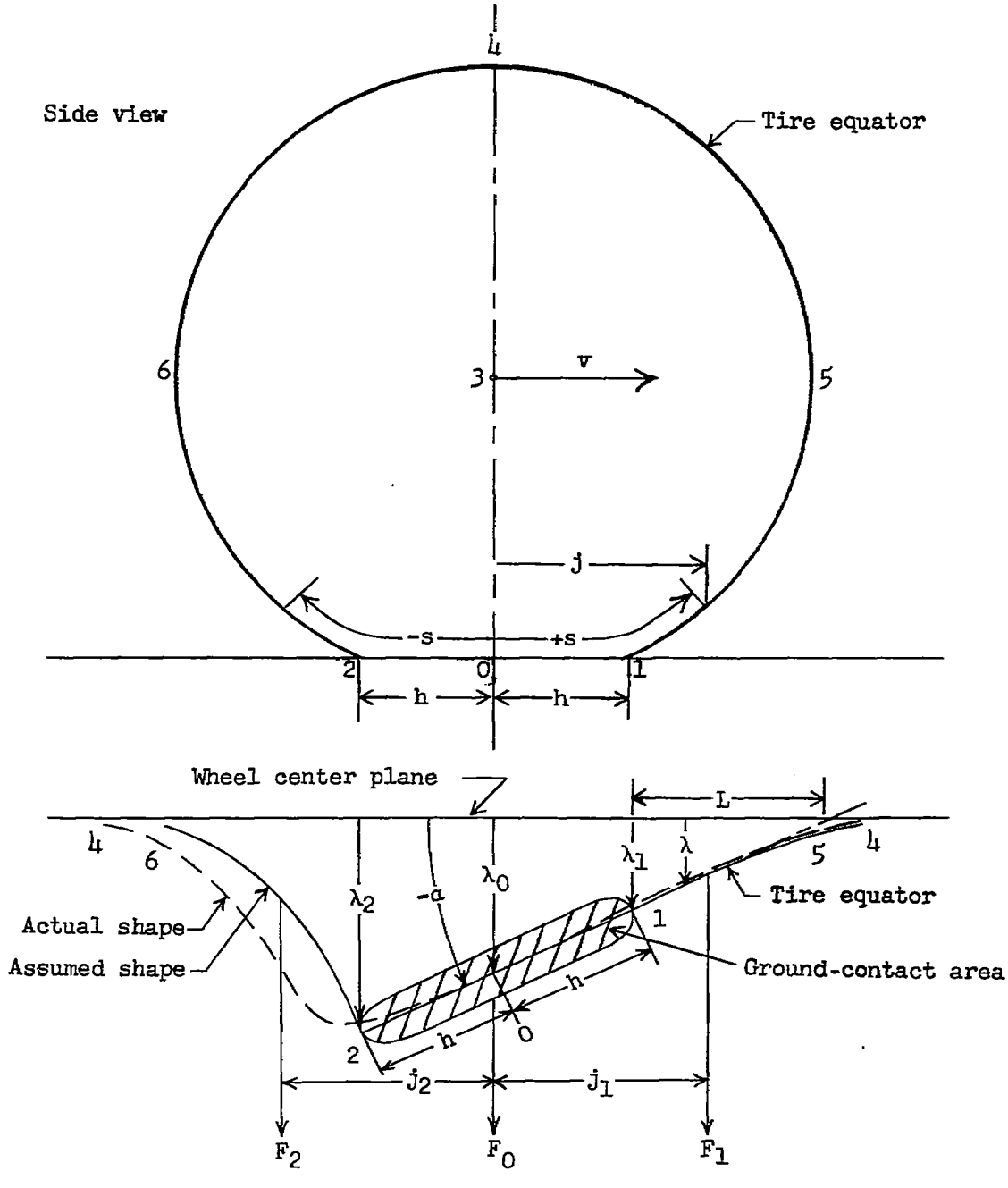

Bottom view
(Tire equator developed onto ground plane)

Figure 1.- Sketch illustrating tire distortion.

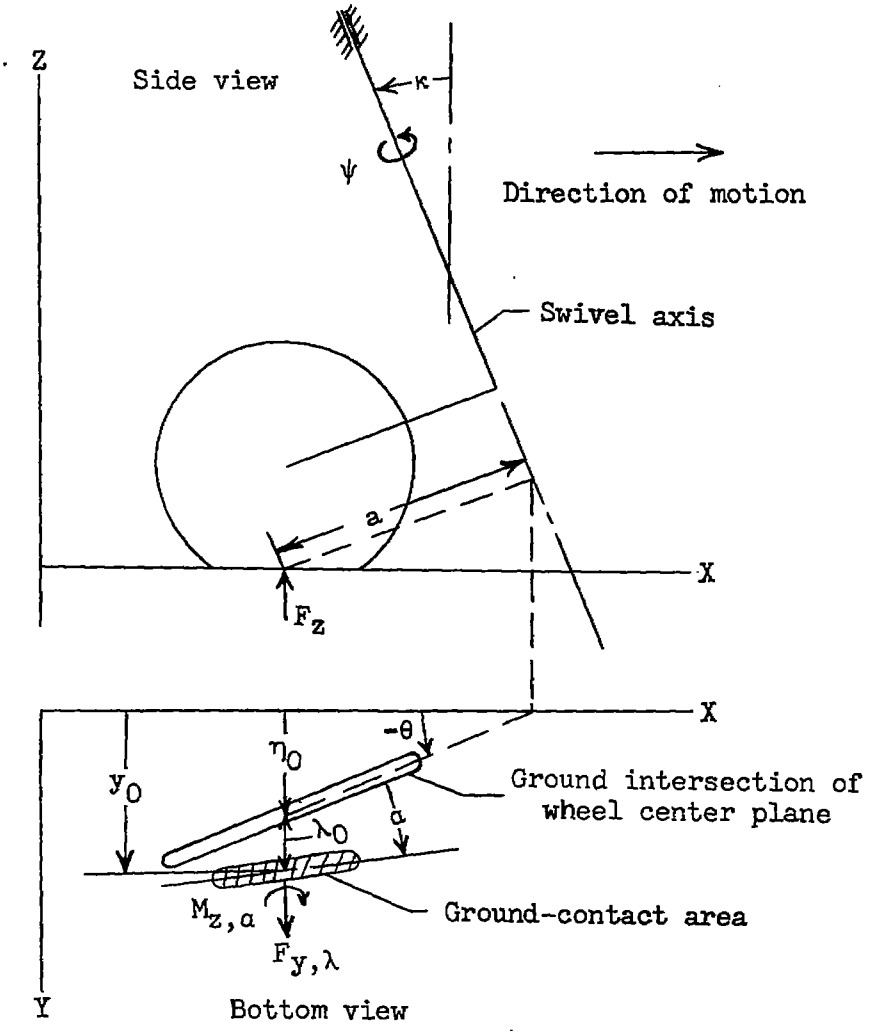

Figure 2.- Configuration of landing gear.

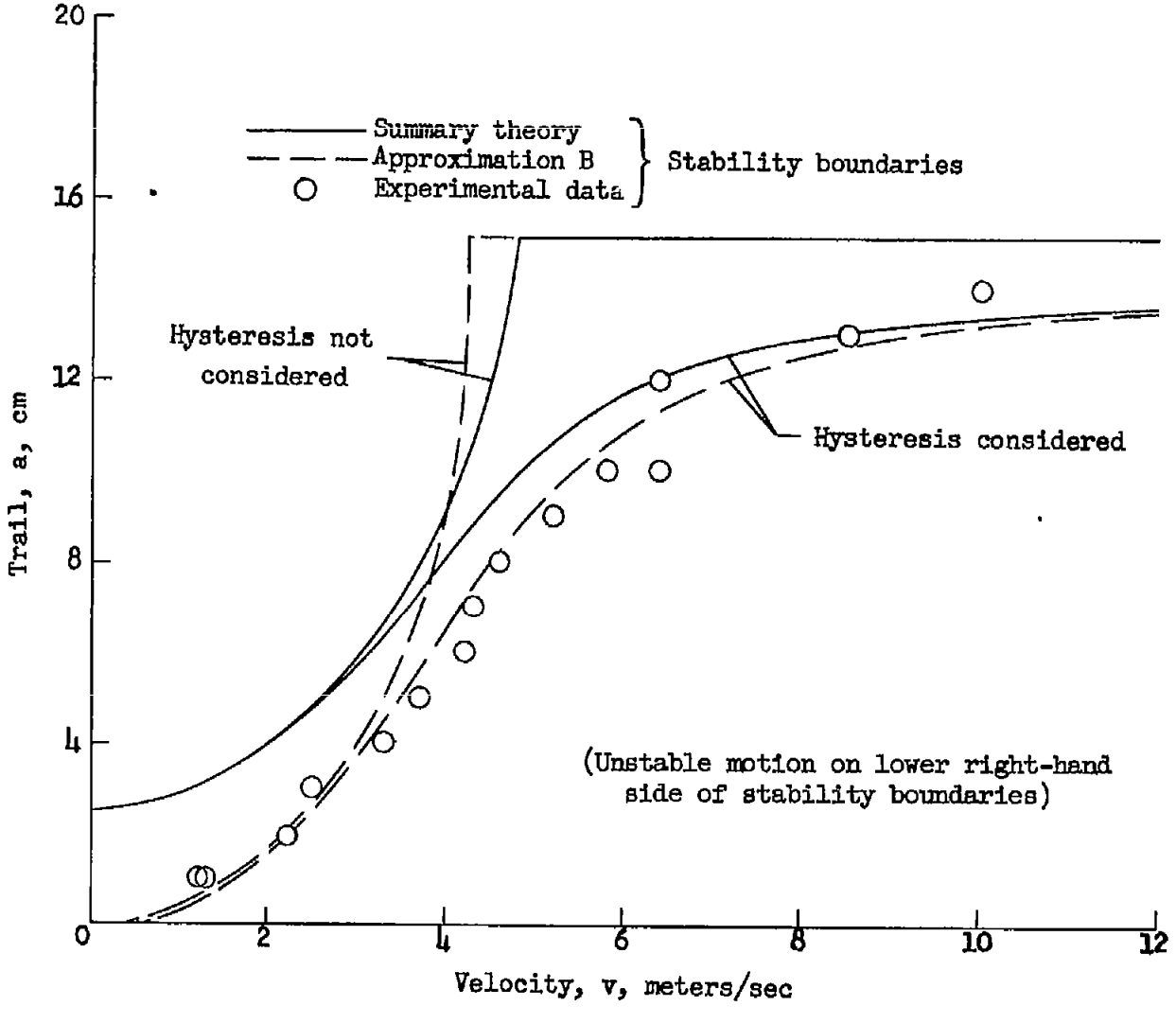

Figure 3.- Effects of hysteresis on the stability boundaries for the Von Schlippe-Dietrich test model of references 2, 8, and 9.

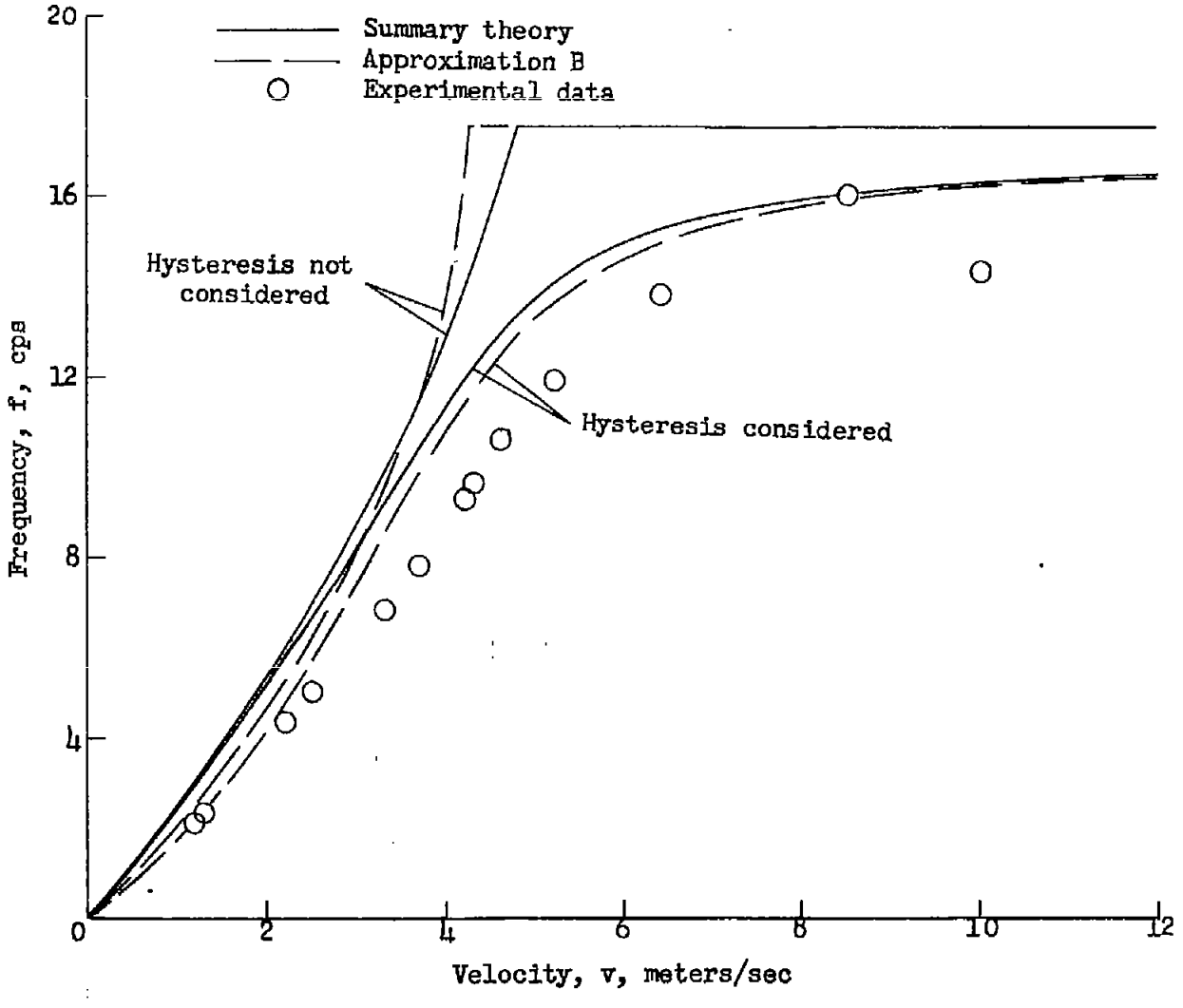

Figure 4.- Effects of hysteresis on the shimmy frequency for the Von Schlippe-Dietrich test model of references 2, 8, and 9.

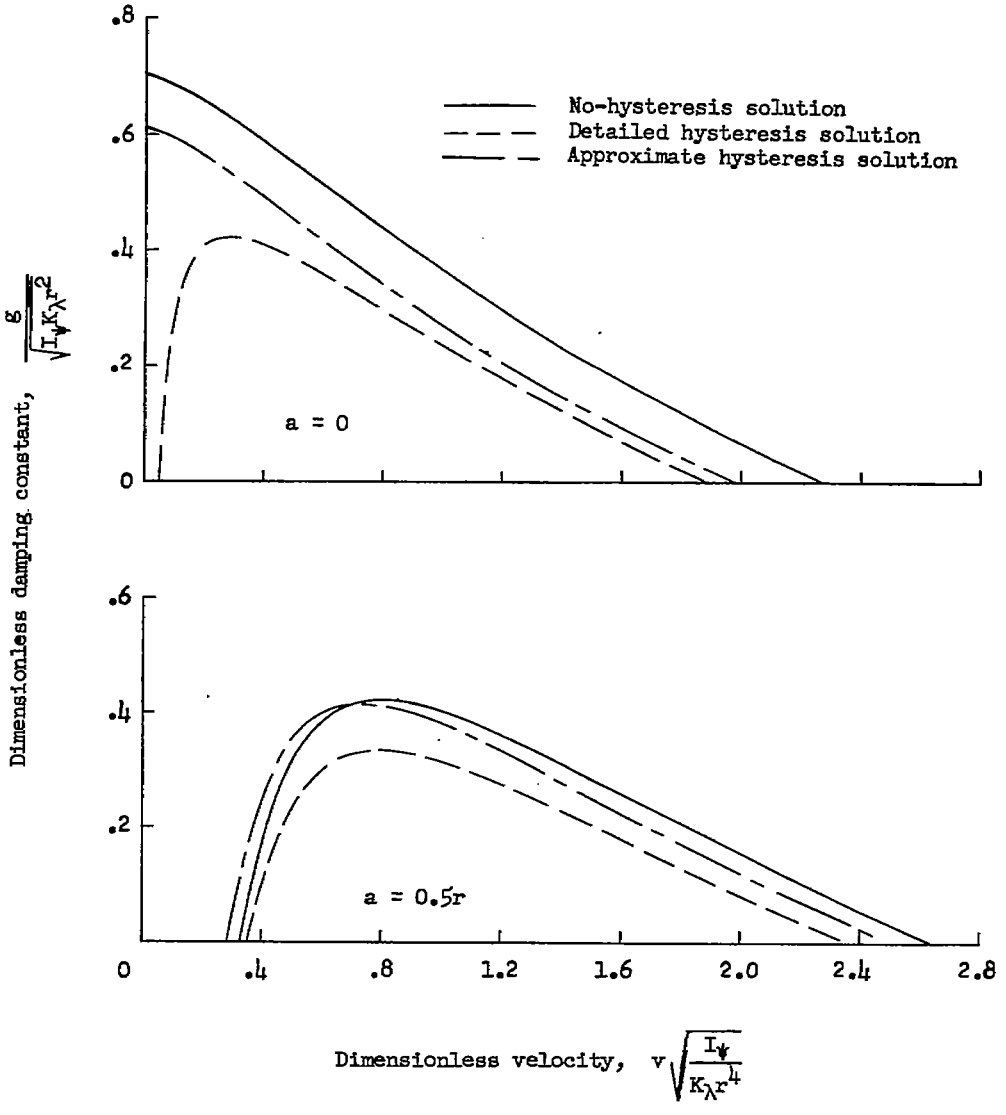

Figure 5.- Influence of velocity and trail on the minimum damping required for stability of a hypothetical landing gear.